optica

Flexible photonic metastructures for tunable coloration

Li Zhu, Jonas Kapraun, James Ferrara, and Connie J. Chang-Hasnain*

Department of Electrical Engineering and Computer Science, University of California Berkeley, Berkeley, California 94720, USA

**Corresponding author: cch@berkeley.edu*

Received 1 October 2014; revised 2 December 2014; accepted 9 December 2014 (Doc. ID 224134); published 12 March 2015

The ability to actively control the perceived color of objects is highly desirable for a variety of applications, such as camouflage, sensing, and displays. We report a completely new flexible, high-contrast metastructure (HCM) whose color can be varied by stretching the membrane. This is accomplished by annihilating the 0th order diffraction while enhancing the -1st order, a new phenomenon made possible with a large index contrast. The color perception of the HCM can thus be changed by varying its period. The structure is fabricated using silicon metastructures embedded in a flexible membrane. We experimentally demonstrate brilliant colors and change the color from green to orange (39 nm wavelength change) with a stretch of 25 nm period change. The same effect can be used for steering a laser beam, with more than 36 resolvable beam spots being demonstrated.

OCIS codes: (160.3918) Metamaterials; (050.6624) Subwavelength structures; (130.5990) Semiconductors; (120.2040) Displays.

http://dx.doi.org/10.1364/OPTICA.2.000255

The conventional optical coating relies on accumulative interference across multiple layers to provide high reflection or transmission of specific wavelengths and, thereby, display a corresponding coloration [1]. Such a structure cannot be used for complex color patterns due to the difficulty in controlling the thickness with fine resolution [2]. Diffractive optics offers another way to split colors. While the 0th order diffraction simply follows Snell's law for reflection and refraction and does not split colors, high-order diffractions have varied propagation directions depending on wavelength. By creating a periodic structure in an elastomeric membrane, control over color perception can be achieved by varying the structural periodicity via membrane deformation. Color tuning has been achieved with the deformation of the elastomeric gratings [3–8]. However, the previously reported structures are made of low-index materials and have a very large proportion of optical power concentrated in the 0th order beam. The typical diffraction efficiency at the desired order is less than 10%. The metal coating on the polymer grating helps to improve the efficiency up to 57% for the near-infrared wavelength [3]. However, it is still much lower than unity. In addition, the metal coating is also not optimal for all colors.

Recently, high-contrast metastructures (HCMs) have emerged as a new optical platform with many designable, extraordinary optical properties [9–14]. HCMs are periodic structures made of one single-layer, high-refractive-index material fully surrounded by low-index material, and a periodicity of nearly one wavelength. Theoretical and experimental works have shown superior performance with new functionalities, such as ultra-broadband high-reflectivity mirrors, high-numerical-aperture lenses, and surface-normal resonators [9,11,14]. In this work, we propose and demonstrate a new HCM structure with nearly all optical power concentrated in the -1st order reflection, or transmission. The enhancement for the -1st diffraction order creates an anomalous reflection, or refraction, at the metastructure interface. In fact, we show that solutions can be found to enhance any of the diffraction orders while suppressing the rest, due to abrupt and large index contrast. This is the first time, to our knowledge, such a phenomenon is observed from a planar periodic diffractive structure. We show that by transferring the HCM from a rigid substrate to a flexible membrane, the HCM becomes highly effective for color change with small deformation.

We designed the metastructures to exhibit green, yellow, orange, and red colors as a color palette, as well as an example display of flower patterns. The measurements show that the power in the -1st order diffraction is more than 15 times stronger than in the 0th order, and the color control agrees well with the simulation.

The schematic of the flexible metastructure is shown in Fig. 1(a). A layer of the HCM consists of an array of pixels

embedded in a transparent, flexible polydimethylsiloxane (PDMS) membrane [15]. The display color variation of the pixels depends solely on the HCM geometry in each pixel, which is defined by a single photolithography step. Figure 1(b) illustrates the configuration of a one-dimensional HCM. The high-index material (n_{bar}) is fully surrounded by low-index material (n_0). Although many materials can be considered as metastructure elements, semiconductors are excellent candidates due to their high index of refraction and fabrication precision [16]. The incident light in the vertical plane perpendicular to the high-index bars is diffracted by the metastructure, with the diffraction angle determined by the well-known grating equation $\Lambda(\sin\theta_i + \sin\theta_m) = m\lambda$. Here, λ, Λ, θ_i, and θ_m are incident wavelength, grating period, incidence angle, and mth order diffraction reflection angle, respectively. When $\Lambda \sim \lambda$, at oblique incidence, there exists a range of θ_i where **two and only two** diffraction orders are allowed. The reflection and transmission coefficients are noted as R_{-1} and R_0, and T_{-1} and T_0, respectively. The analytical solution for the HCM with abrupt and large index contrast is described in Ref. [14]. Here, we extend the solution for diffraction efficiency to higher orders. We consider the HCMs as a periodic array of waveguides along the z direction. Upon plane wave incidence, a few waveguide array modes are excited. After propagating through the HCM thickness, each mode possesses a different phase. At the exiting interface, due to the strong mismatch to the existing plane wave, the waveguide modes not only reflect back to themselves but also couple to each other. As the modes return to the input plane, similar coupling occurs. Following the modes through one roundtrip,

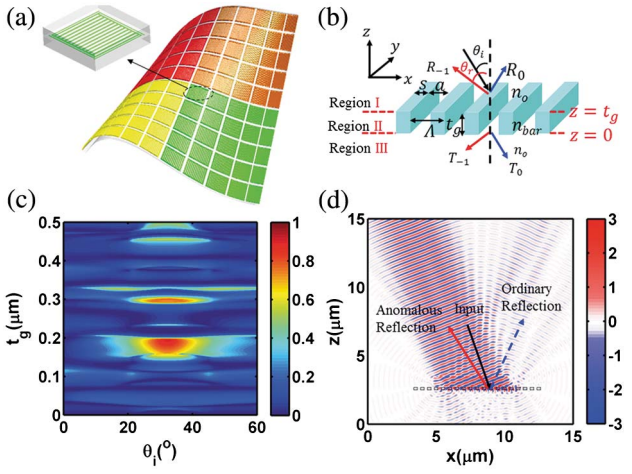

Fig. 1. (a) Schematic of the color display from the HCM embedded flexible membrane. The display pattern is composed of individual pixels with a designed color. One pixel consists of an HCM with nanoscale features, which is very flexible and robust to deformation. (b) Schematic of a one-dimensional HCM. The optical properties are determined by three key parameters: period Λ, thickness t_g, and duty cycle $\eta = \frac{s}{\Lambda}$, where s is the width of the high-index bar. In the two-order diffraction regime, the incident light is diffracted into four possible orders: R_{-1}, R_0, T_{-1}, and T_0. (c) R_{-1} with varied t_g and incidence angle θ_i for HCM design with 500 nm period and 0.5 duty cycle at 532 nm wavelength. (d) FDTD simulation of the anomalous reflection phenomenon for the HCM design in (c) with 180 nm thickness and 32° incidence angle.

Table 1. Design Parameters for the Four-Color Palette

Design	A	B	C	D
Intended Color	Green	Yellow	Orange	Red
Peak R_{-1} Wavelength (nm)	540	570	590	630
Period (nm)	500	532	558	622
Duty Cycle	0.5	0.5	0.5	0.5
Thickness (nm)	180	180	180	220

the reflectivity and transmission can be solved for any of the diffraction orders. We find that solutions can be found to enhance *any* of the diffraction orders while suppressing the rest.

An anomalous reflection or refraction at the metastructure interface can be attained with the enhancement of R_{-1} or T_{-1} while eliminating the rest. For an HCM design with fixed period and duty cycle, R_{-1} is calculated with varied thickness and incidence angle for 532 nm wavelength, as shown in Fig. 1(c). **Close to 100% diffraction efficiency** is obtained for R_{-1}, leading to anomalous reflection over a wide range of incidence angles. Figure 1(d) shows the optical field of a metastructure made of silicon designed for 532 nm wavelength simulated by the finite-difference time-domain (FDTD) method [17]. Under such configuration, the output light propagates toward the side of incidence, in sharp contrast to what is governed by Snell's law. This is the first time, to our knowledge, such a phenomenon is observed with a planar periodic diffractive structure.

In this work, we focus our experimental demonstration on anomalous reflection at the visible wavelengths for controllable coloration of TE-polarized incident light. However, the design rules can be applied to TM-polarized or even unpolarized light. Furthermore, an HCM can also be designed for anomalous refraction. We chose silicon as the high-index material in the demonstration despite absorption in the visible wavelengths due to the availability of high-precision fabrication.

Figure 2(a) shows the main steps for the fabrication process. A silicon-on-insulator wafer is used. Various colors can be achieved with the same silicon layer thickness but different HCM dimensions, as listed in Table 1. To facilitate the transfer to a flexible substrate, the HCMs are made into a pixel array with 100 μm pitch and 92% filling factor. In addition, to support the HCM in the release step, a large frame with folded beams is used to connect the HCM pixels. The HCMs are patterned by deep ultraviolet (DUV) step-lithography followed by a silicon etch. The top and cross-section view SEM images of the etched silicon features are shown in Fig. 2(b). The inset figure defines the key geometry of an HCM design. The HCM structure is subsequently released by etching away the SiO_2 layer, and transferred with a PDMS stamp [18]. A second PDMS stamp is used to encapsulate the HCM for added protection. For convenience during the deformation measurement, the final thickness of the PDMS sample is on the order of 1 mm. The detail of the fabrication process is presented in Supplement 1. Figure 2(c) shows microscopic (left) and SEM images (right) of transferred HCMs on PDMS before encapsulation. Very high transfer yield can be achieved with this technique. As shown in Fig. 2(c), the entire 1 cm × 1 cm sample does not have a single bad pixel.

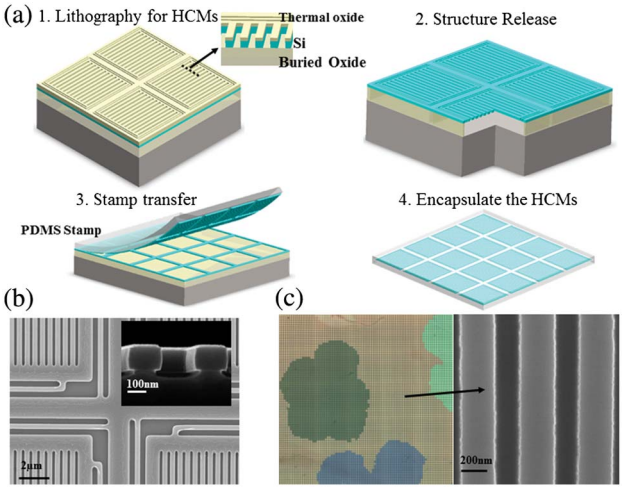

Fig. 2. (a) Schematic of the major steps for fabrication. Step 1: Etching the silicon metastructure with the thermal oxide as the hard mask; the inset shows the cross-section of the etching profile. Step 2: Release the HCMs from the substrate with vapor hydrofluoric acid etching. Step 3: Use stamp transfer method to transfer the silicon HCMs to the PDMS membrane. Step 4: Encapsulate the flexible HCM sample with PDMS. (b) Scanning electron microscope (SEM) images for the HCM on silicon on insulator after etching. The inset shows the cross-section. (c) Microscopic (left) and SEM (right) images for the transferred HCMs on PDMS before encapsulation. The left image is a large 1 cm × 1 cm sample. Each individual pixel is 100 μm × 100 μm size. The right image is the top-view SEM of the HCM.

Design A (intended for green color) is measured using 532 nm wavelength laser illumination and detected by a large area photodiode. Figure 3(a) shows R_{-1} and R_0 as a function of incidence angle. As high as 83% diffraction efficiency in the -1st reflection order (R_{-1}) is obtained, 15.4 times stronger than R_0. The theoretical R_{-1} value, including residual absorption in Si at 532 nm, is 88.3%. The measured value is slightly lower, mainly attributed to the nonvertical and rough sidewalls of the HCM. These can be improved with various methods, such as UV resist reflow, and through the use of a hard mask with better selectivity, such as Si_3N_4. The incidence angle dependence of the diffraction can be mitigated by apodizing the HCMs. Using the method in [11], the diffraction can be designed to be less sensitive to the incidence angle. The reflection angle of the diffracted coherent light can be steered by stretching the flexible membrane. As shown in Fig. 3(b), a 5.5° irradiation angle is steered by 5.45% deformation, which is defined as the ratio of the change of length over the original length $\varepsilon = \Delta L/L$. The full width half maximum of the beam remains unchanged at 0.3°, while the optical power change remains within 3 dB. This represents more than 36 resolvable spots. Such a result shows that a flexible HCM can be excellent for beam-steering applications.

Vivid colors are achieved when the samples are under white light illumination, as shown by the photographs in Figs. 3(c) and 3(d). A 16 mm × 16 mm flower pattern image designed to show five colors, including the primary color set, is shown

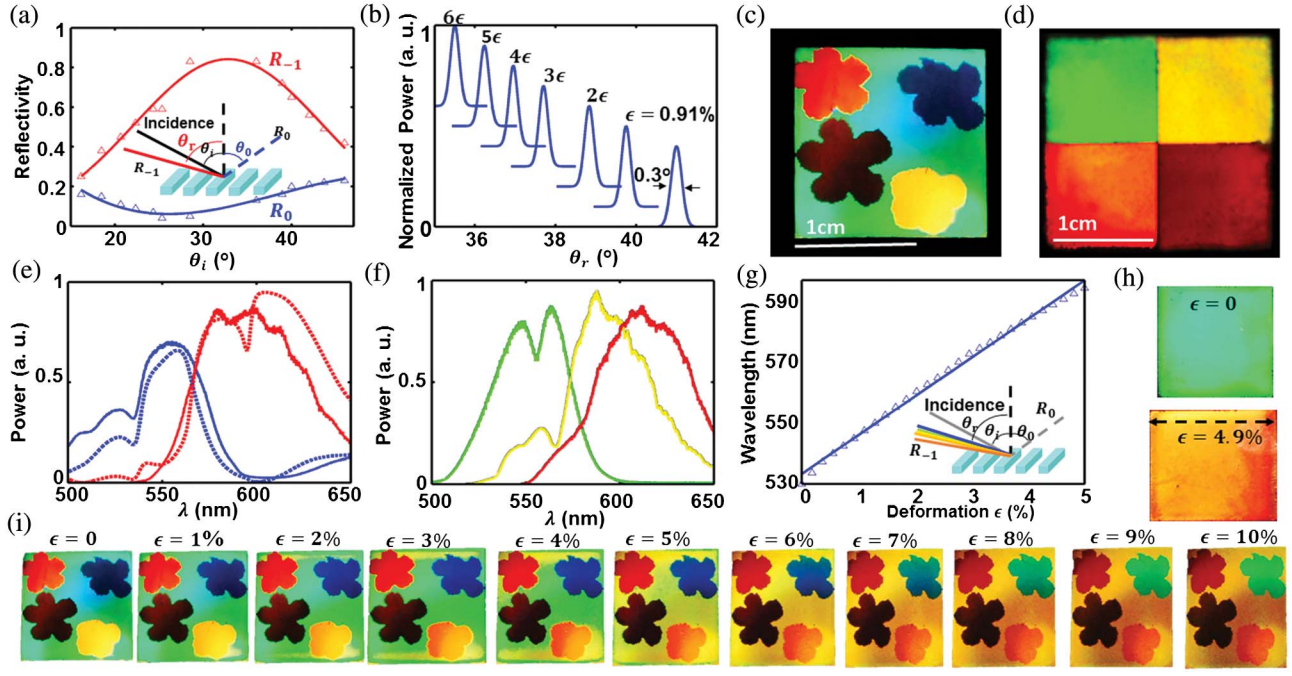

Fig. 3. (a) Reflectivity dependence on the incidence angle for the green HCM design measured with a 532 nm green laser. (b) Beam steering effect characterization within a 3 dB optical power range. The flexible membrane is illuminated by a green laser. The irradiation angle of R_{-1} is steered with the stretching of the membrane. (c) Photograph of the display sample under the white light illumination. (d) Photograph of the four colors (green, yellow, orange, and red) as the color palette under the white light illumination. (e) Normalized spectra of the measurement (solid lines) and simulation (dashed lines) results for Design C. Red and blue curves represent the -1st order and 0th order, respectively. (f) Spectra of the -1st order for green, yellow, and red designs. (g) Color control effect characterization for the green HCM design in the 3 dB peak power range. The spectrum is measured at the fixed incidence and perception angle. By stretching the flexible membrane, the peak shifts to longer wavelengths. (h) Photographs of the sample before ($\varepsilon = 0$) and after ($\varepsilon = 4.9\%$) stretching. Media 1 (i) Photos of the flower pattern under different deformation.

in Fig. 3(c). The color-rendering sample agrees well with the design. Figure 3(d) shows a 20 mm × 20 mm sample with a four-color palette, designed for quantitative characterization. The design rationale and simulations are described in Supplement 1. The blue color design with greater than 80% efficiency exceeds our 258 nm DUV stepper resolution and is therefore not fabricated in this demonstration. However, it can be achieved with lower efficiency, as shown in Fig. 3(c). The geometry parameters of the color palette are listed in Table 1. The diffraction spectra of all four designs are measured with white light illumination. A fiber-coupled white LED irradiates the HCM sample through a collimator with 0.05° divergence angle. The diffracted light is collected by another collimator and coupled into the visible light spectrometer. The detailed configuration of the measurement setup is discussed in Supplement 1. Figure 3(e) shows measured (solid lines) and simulated R_{-1} and R_0 spectra (dashed lines) for Design C. Both the -1st and 0th order reflection spectra achieve excellent agreement with the theoretical prediction. At the designed peak wavelength (590 nm), the power at the -1st order dominates the diffraction. Figure 3(f) shows the measured spectra of R_{-1} for the rest of the colors, green, yellow, and red. The strong peak power is verified at the designed wavelength.

Color perception can be controlled by stretching the flexible membrane. The resulting deformation varies the low-index gap size and therefore changes the periodicity of the metastructure. Under a fixed input and output angle, the control of the HCM period leads to the control of the perceived color. The quantitative characterization is shown in Fig. 3(g), where the spectra with varied deformation are plotted. By stretching the green HCM sample by $\varepsilon = 4.9\%$, which corresponds to only a 25 nm change of the HCM period, the measured wavelength has already shifted by 39 nm, from 541 to 580 nm, leading the display color to be changed from green to orange while the optical power still remains within 3 dB. Additional stretching can further extend the color tuning range. However, the diffraction efficiency tends to decrease as the low index gap increases, as shown in Fig. S3 in Supplement 1. The sample contraction in the direction perpendicular to the stretching can also cause the efficiency to drop when $\varepsilon > 10\%$ from observation. This effect can be optimized using a two-dimensional grating structure. The photographs of the sample before and after stretching are shown in Fig. 3(h) for Design A. Such an effect is also presented in Media 1. The color at the relaxed state shows excellent uniformity due to the uniform fabrication across the large sample. Less than 10 nm wavelength variation is observed after stretching, which is mainly due to nonuniform applied force from the current setup and the imperfection from the PDMS polymerization step for sample encapsulation. Figure 3(i) shows the color changes of different designs that can be simultaneously achieved. This result demonstrates that the displayed color can be designed to be very sensitive to deformation, for instance, deep blue changes to green, vermilion changes to carmine, yellow changes to orange, and cyan background changes to yellow; or, it can be designed to remain unchanged with stretching, as the black flower shown in Fig. 3(i).

In conclusion, we have discovered a completely new phenomenon, to our knowledge, for a planar periodic diffractive structure which exhibits anomalous reflection and refraction. We demonstrate the first flexible semiconductor metastructure and use it for active coloration. Excellent figures of merit and agreement with theoretical predictions have been achieved with the chosen implementation. Greater than 99.9% process yield is achieved for macroscale samples, making this approach very suitable for large-volume production. With the flexibility of a PDMS membrane, an HCM can be coated on the surface of objects, making a color display sensitive to geometrical change. Based on the large amount of reports regarding PDMS for MEMS applications, we expect excellent repeatability for a large number of stretching cycles. The minimum requirement for a single-pixel HCM is two periods, which can transcend state-of-the-art displays below single micrometer resolution. The results presented here provide an illustration of the opportunities available for utilizing HCMs in flexible optics applications, ranging from camouflage and the visual arts at the macroscale, down to biolabeling and imaging at the microscale.

FUNDING INFORMATION

Alexander von Humboldt Foundation; National Science Foundation (NSF) (0939514); U.S. Department of Defense (DOD) (N00244-09-1-0013, N00244-09-1-0080); UC Multicampus Research Program and Initiatives (MRPI).

See Supplement 1 for supporting content.

REFERENCES

1. H. A. Macleod, in *Thin-film Optical Filters* (Adam Hilger, 1986).
2. M. Kolle, B. Zheng, N. Gibbons, J. Baumberg, and U. Steiner, Opt. Express **18**, 4356 (2010).
3. S. Bertani, B. Jacobsson, F. Laurell, V. Pasiskevicius, and M. Stjernstrom, Opt. Express **14**, 11982 (2006).
4. M. Aschwanden and A. Stemmer, Opt. Lett. **31**, 2610 (2006).
5. K. Suzumori, M. Mihara, and S. Wakimoto, in *IEEE International Conference on Robotics and Automation* (IEEE, 2001), p. 2771.
6. H. Fudouzi and T. Sawada, Langmuir **22**, 1365 (2006).
7. Z. H. Fang, C. Punckt, E. Y. Leung, H. C. Schniepp, and I. A. Aksay, Appl. Opt. **49**, 6689 (2010).
8. C. E. Finlayson and J. J. Baumberg, Polym. Int. **62**, 1403 (2013).
9. C. F. R. Mateus, M. C. Huang, Y. Deng, A. R. Neureuther, and C. J. Chang-Hasnain, IEEE Photon. Technol. Lett. **16**, 518 (2004).
10. M. C. Y. Huang, Y. Zhou, and C. J. Chang-Hasnain, Nat. Photonics **1**, 119 (2007).
11. F. Lu, F. G. Sedgwick, V. Karagodsky, C. Chase, and C. J. Chang-Hasnain, Opt. Express **18**, 12606 (2010).
12. W. Yang, J. Ferrara, K. Grutter, A. Yeh, C. Chase, Y. Yue, A. E. Willner, M. C. Wu, and C. J. Chang-Hasnain, Nanophotonics **1**, 23 (2012).
13. C. J. Chang-Hasnain and W. Yang, Adv. Opt. Photon. **4**, 379 (2012).
14. Y. Zhou, M. C. Huang, C. Chase, V. Karagodsky, M. Moewe, B. Pesala, F. G. Sedgwick, and C. J. Chang-Hasnain, Opt. Express **16**, 17282 (2008).
15. J. C. Lotters, W. Olthuis, P. H. Veltink, and P. Bergveld, J. Micromech. Microeng. **7**, 145 (1997).
16. A. J. Hoffman, L. Alekseyev, S. S. Howard, K. J. Franz, D. Wasserman, V. A. Podolskiy, E. E. Narimanov, D. L. Sivco, and C. Gmachl, Nat. Mater. **6**, 946 (2007).
17. S. K. Kunz and R. J. Luebbers, in *The Finite Difference Time Domain Method for Electromagnetics* (CRC Press, 1993).
18. M. A. Meitl, Z. T. Zhu, V. Kumar, K. J. Lee, X. Feng, Y. Y. Huang, A. Ilesanmi, R. G. Nuzzo, and J. A. Rogers, Nat. Mater. **5**, 33 (2006).